

Removal of Congo Red from Aqueous Solution Using Magnetic Chitosan Composite Microparticles

Peng Wang, Tingguo Yan, and Lijuan Wang*

Magnetic chitosan composite microparticles (MCCPs) were successfully prepared using a simple one-step co-precipitation method and characterized by scanning electron microscopy (SEM), X-ray diffraction (XRD), Fourier transform infrared spectroscopy (FT-IR), and vibrating sample magnetometer (VSM). The experimental results showed that the particles possessed a honeycomb-like porous structure and had superparamagnetic properties, with a saturation magnetization of about 33.3 emu/g. Congo red (CR), an anionic azo dye, was used to investigate the adsorption properties of the MCCPs. The adsorption kinetics data and isotherms produced from these experiments indicated that CR adsorption onto the MCCPs was best fitted with a pseudo-second-order kinetic equation and was well described by the Langmuir model. Thermodynamic parameters such as the changes in Gibbs free energy (ΔG°), enthalpy (ΔH°), and entropy (ΔS°) were also estimated; the results revealed that the adsorption process was spontaneous and endothermic. The regeneration studies demonstrated that the MCCPs can be used as a reusable adsorbent for CR adsorption from aqueous solution. The molecular similarity between chitosan and cellulose suggests that the present results might serve as a model of what might be achieved with a cationic derivative of cellulose.

Keywords: Chitosan; Fe_3O_4 ; Magnetic microparticles; Removal; Congo red; Regeneration

Contact information: Key Laboratory of Bio-based Material Science and Technology of Ministry of Education, Northeast Forestry University, 26 Hexing Road, Harbin 150040, China;

*Corresponding author: donglinwlj@163.com

INTRODUCTION

The large quantities of dyes discharged from the textile, clothing, and printing industries are major sources of aquatic pollution. Most of these dyes are very colorful, but have high biochemical and chemical oxygen demands, smell unpleasant, and are toxic (Crini and Badot 2008). These toxic effluents can cause considerable damage to human and marine life if they are not treated prior to discharge. Unfortunately, dyes are rather difficult to remove from wastewater because of their synthetic origins and complex aromatic structures (Srinivasan and Viraraghavan 2010). Several physical, chemical, and biological techniques have been used to remove dyes from wastewater. These techniques include coagulation (Shi *et al.* 2007), chemical treatment (Wang *et al.* 2007; Mishra and Bajpai 2006), oxidation (Hage and Lienke 2005; Ertugay and Acar 2013), electrochemical methods (Gupta *et al.* 2007; Dogan and Türkdemir 2005), biological treatment (Barragán *et al.* 2007; Bromley-Challenor 2000; Sani and Banerjee 1999), adsorption, and ion exchange (Liu *et al.* 2007; Raghu and Ahmed Basha 2007). Among them, adsorption is considered to be an effective and versatile method for removing dyes from aqueous solutions. Activated carbon is an effective adsorbent, but it is too expensive

for practical use. Many researchers have studied the feasibility of low-cost, natural materials for dye removal, such as wood, natural coal, peat, clays, and silica (Srinivasan and Viraraghavan 2010; Gupta *et al.* 2009; Morais *et al.* 1999; Venkata Mohan *et al.* 2002; Sun and Yang 2003). However, these low-cost adsorbents generally have low adsorption capacities. Thus, there is still a need to find economical, easily available, and highly effective alternative adsorbents.

Chitosan is a type of natural polyaminosaccharide obtained from chitin partial deacetylation; it is the second-most abundant polymer in nature after the lignocellulose group (Wan Ngah *et al.* 2011). It can be extracted from the shells of prawns, crabs, fungi, insects, and other crustaceans (Ngah and Isa 1998). The carbohydrate backbone of chitosan is very similar to that of cellulose; chitosan may be regarded as cellulose with the hydroxyl at position C-2 replaced by an amino group. Thus, chitosan is a copolymer consisting of N-acetyl-2-amino-2-deoxy-D-glucopyranose, where the two types of repeating units are linked by (1→4)- β -glycosidic bonds. It can therefore serve as a model for what might be done with cellulose-based polymers.

Recent studies demonstrate that cationic cellulose derivatives have many useful characteristics, such as hydrophilicity, biodegradability, antibacterial properties, and dyeability. Rodríguez *et al.* (2003) synthesized cationic cellulose hydrogels and evaluated their utility for controlling the release of an anionic amphiphilic drug, diclofenac sodium. Jia *et al.* (2011) reported the preparation of nano-fiber mats with antibacterial activity by electrospinning of a blended solution of cationic cellulose derivates and polyvinyl alcohol. Khatri *et al.* (2013) prepared cationic cellulose nanofibers for enhanced color yields and dye fixation. Sirviö *et al.* (2011) reported the synthesis of a highly cationic water-soluble cellulose derivative as a novel biopolymeric flocculation agent.

Chitosan, regarded as a kind of cationic cellulose derivative, exhibits a high adsorption capacity for many classes of dyes. However, powdery chitosan has some disadvantages that frustrate its use in practical applications; it is easily dissolved under acidic conditions and has poor mechanical strength (Zhu *et al.* 2010). Many studies have investigated the use of various materials to form chitosan composites; these materials include montmorillonite, polyurethane, activated clay, bentonite, oil palm ash, and kaolin (Wang and Wang 2007b; Lin *et al.* 2004; Lee *et al.* 2009; Nandi *et al.* 2009). However, the separation and recovery of them are still problematic for researchers.

Magnetic separation technology is a promising method to separate powdery adsorbents from the adsorbed solution effectively and in an environmentally friendly way. In recent years, many studies have reported on removing dyes (Fan *et al.* 2013; Travlou *et al.* 2013; Yan *et al.* 2013; Yan *et al.* 2012; Yang *et al.* 2013; Zhu *et al.* 2012) and metal ions (Kyzas and Deliyanni 2013; Abou El-Reash *et al.* 2011; Donia *et al.* 2008; Elwakeel 2010; Li *et al.* 2011; Yu *et al.* 2013) using magnetic chitosan composite adsorbents. To prepare magnetic chitosan composites, most of the researchers have applied a two-step method based on the inverse emulsion process (Lee *et al.* 2005; Fan *et al.* 2012b; Qu *et al.* 2010; Li *et al.* 2008). However, it is not known if more than a few researchers have reported preparing a Fe₃O₄/chitosan composite using a one-step approach and using it to remove dyes from an aqueous solution.

In this work, magnetic chitosan composite microparticles (MCCPs) were prepared using a facile one-step *in situ* co-precipitation process, then characterized by scanning electron microscopy (SEM), X-ray diffraction (XRD), Fourier transform infrared spectroscopy (FT-IR), and vibrating sample magnetometer (VSM). Congo red (CR), which has a large and complicated structure, was used as a model dye for bath adsorption

experiments to investigate the adsorption properties of the MCCPs. The effects of the solution pH and initial dye concentration on CR adsorption were investigated. Adsorption kinetics was evaluated with Lagergren pseudo-first-order and pseudo-second-order models. Equilibrium isotherms and thermodynamic parameters were also determined and will be discussed. These results will be useful for further applications involving dye removal from aqueous solutions.

EXPERIMENTAL

Materials

Chitosan (Deacetylation Degree: 85%; Molecular Weight: 3.0×10^5 g mol⁻¹) was purchased from Sinopharm Chemical Reagent Co., Ltd., China. CR (Molecular Weight: 696.68; C₃₂H₂₂N₆O₆S₂Na₂; Color index No.: 22120; Purity: 85%) was purchased from Tianjin Bodi Chemical Co., Ltd., China. The FeCl₃·6H₂O, FeSO₄·7H₂O, and glutaraldehyde compounds used were of analytical grade and supplied by Tianjin Kermel Chemical Reagent Co., Ltd., China. A stock solution of Congo red (1000 mg L⁻¹) was prepared in double-distilled water; desired CR solution concentrations were obtained by successive dilutions of the stock solution.

Preparation of MCCPs

Magnetic chitosan microparticles were prepared by a one-step co-precipitation method (Tran *et al.* 2010; Liu *et al.* 2011). First, 1.5 g of chitosan was dissolved overnight in 100 mL of 2% (v/v) acetic acid solution. Afterwards, 0.03 mol FeCl₃·6H₂O and 0.018 mol FeSO₄·7H₂O were added into the solution, which was stirred for 30 min. The resulting solution was dripped into a 30 wt.% NaOH solution under vigorous stirring at 60 °C in an N₂ atmosphere. After 6 h of reaction, the suspension was magnetically separated and washed several times until its pH became neutral. The black products were then dispersed in a 1.0 wt.% glutaraldehyde solution for crosslinking. After 3 h, the final products were separated from the solution and rinsed with ethanol and deionized water three times. The magnetic chitosan composite microparticles were then dried in a vacuum at 70 °C for 24 h.

Characterization of the MCCPs

The morphologies and microstructures of the samples were observed by scanning electron microscopy (SEM, Quanta 200) with an accelerating voltage of 15 kV. The crystal structures of the microparticles were determined by X-ray diffraction (XRD, Rigaku D/max-2200 diffractometer) using Cu K α radiation at 40 kV and 30 mA. FT-IR spectra were measured at room temperature on an FT-IR spectrometer (Nicolet 560) to investigate the functional groups of the microparticles. Magnetic hysteresis loops were obtained at 298 K using a vibrating sample magnetometer (VSM).

Batch Adsorption Experiments

The adsorption of CR on the MCCPs was studied by batch experiments using a thermostatic rotary shaker at 120 rpm. Standard solutions of different concentrations were prepared by diluting the 1000 mg L⁻¹ CR stock solution. For a typical adsorption experiment, 30 mg of MCCPs was mixed with 50 mL of a CR solution at a 50 mg L⁻¹ concentration. At given time intervals, the microparticles were removed from the solution

using an adscititious magnet. The CR concentration in the solution was determined by a UV-vis spectrophotometer at $\lambda_{\text{max}} = 494$ nm. The amount of CR adsorbed on the MCCPs, q_t (mg g^{-1}), was calculated as follows,

$$q_t = \frac{(C_0 - C_t)V}{W} \quad (1)$$

where C_0 and C_t are the initial CR concentration (mg L^{-1}) and instantaneous CR concentration (mg L^{-1}), respectively, V is the volume of the solution (L), and W is the weight of the adsorbent (g).

RESULTS AND DISCUSSION

Characterization of the MCCPs

The morphology and microstructure of the MCCPs were observed using SEM, as shown in Fig. 1. Honeycomb-like porous structures are clearly seen in Fig. 1(a). The shapes of the microparticles are irregular because of aggregation, and their surfaces are relatively rough. Figure 1(b) shows that the pore size was fairly uniform and that the mean pore diameter was about 4 μm . Similar to activated carbon (Tan *et al.* 2007), the well-developed pores present on the surface led to the large surface area and increased the possibility of dye trapping and adsorption.

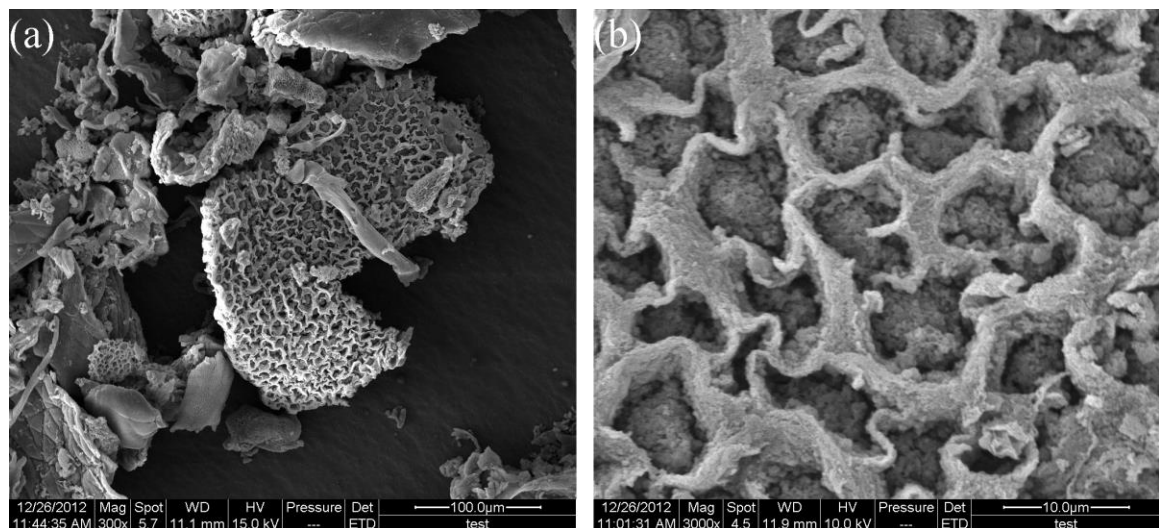


Fig. 1. SEM micrographs of the MCCPs

Figure 2 shows the XRD patterns for the plain Fe_3O_4 microparticles and MCCPs. Six characteristic peaks for Fe_3O_4 at 2θ values of 30.72° , 35.38° , 43.72° , 53.64° , 57.24° , and 62.86° were marked by their corresponding indices: (220), (311), (400), (422), (511), and (440), respectively; these peaks were observed for both samples. These peaks revealed that the particles were pure Fe_3O_4 with a spinel structure (JCPDS database file, No.79-0418). These results also suggest that the Fe_3O_4 in the MCCPs prepared by the one-step co-precipitation process has the same crystal structure as plain Fe_3O_4 .

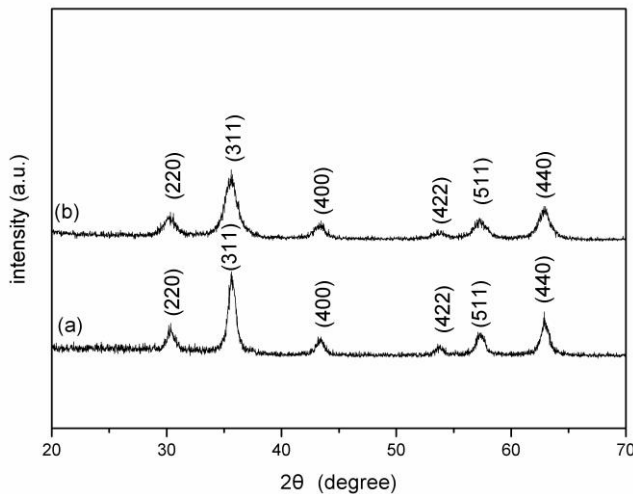


Fig. 2. XRD patterns for naked Fe_3O_4 microparticles (a) and MCCPs (b)

Figure 3 shows the FT-IR spectra of plain Fe_3O_4 , chitosan, and the MCCPs. As Fig. 3(a) shows, the peak at 587 cm^{-1} is related to the Fe-O group (Ma *et al.* 2007). For the FT-IR spectrum of chitosan in Fig. 3(b), the adsorption band around 3330 cm^{-1} is assigned to the $-\text{OH}$ and $-\text{NH}_2$ stretching vibrations. The peaks at 1583 cm^{-1} and 1374 cm^{-1} are ascribed to the N-H bending vibration and $-\text{C}-\text{O}$ stretching of alcoholic groups in chitosan, respectively (Zhang *et al.* 2010). For the MCCPs in Fig. 3(c), the sharp peak at 583 cm^{-1} is from Fe-O stretching of Fe_3O_4 . A new peak at 1631 cm^{-1} is present, which is attributed to an imine bond ($\text{N}=\text{C}$), indicating that the chitosan was successfully cross-linked by the glutaraldehyde (Elwakeel 2010). Additionally, the negatively charged surface of iron oxide has an affinity toward chitosan. This means that protonated chitosan could be coated on the particles by electrostatic interaction and chemical reactions, specifically, glutaraldehyde crosslinking (Lin *et al.* 2010).

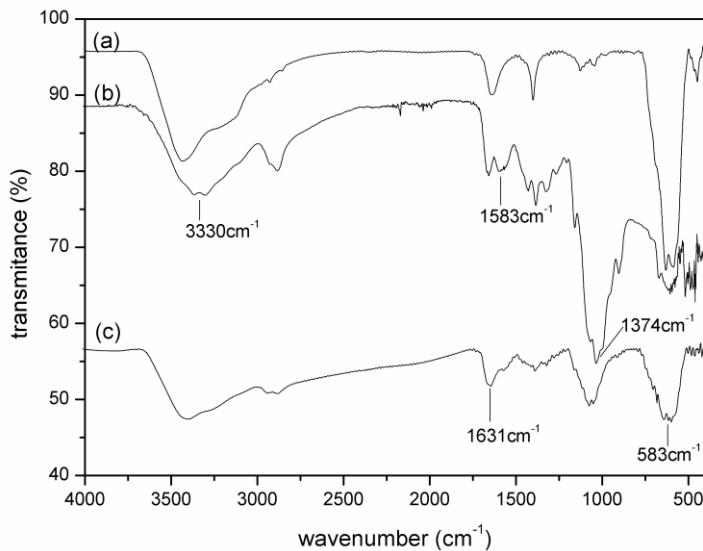


Fig. 3. FT-IR spectra of (a) naked Fe_3O_4 , (b) chitosan, and (c) MCCPs

The magnetic properties of the MCCPs were measured using VSM. Figure 4(a) shows the magnetization hysteresis loop for the MCCPs obtained at 298 K. There was no remanence or coercivity observed, indicating that the particles were superparamagnetic (Li *et al.* 2008). The saturation magnetization of the MCCPs obtained from the hysteresis loop was 33.3 emu/g. Figure 4(b) shows that the MCCPs dispersed well in water before magnetic separation. However, almost all of the MCCPs could be quickly separated from the solution when an external magnetic field was introduced, as shown in Fig. 4(c). These results illustrate that the MCCPs have a sensitive magnetic response, which is important for their use in wastewater treatment.

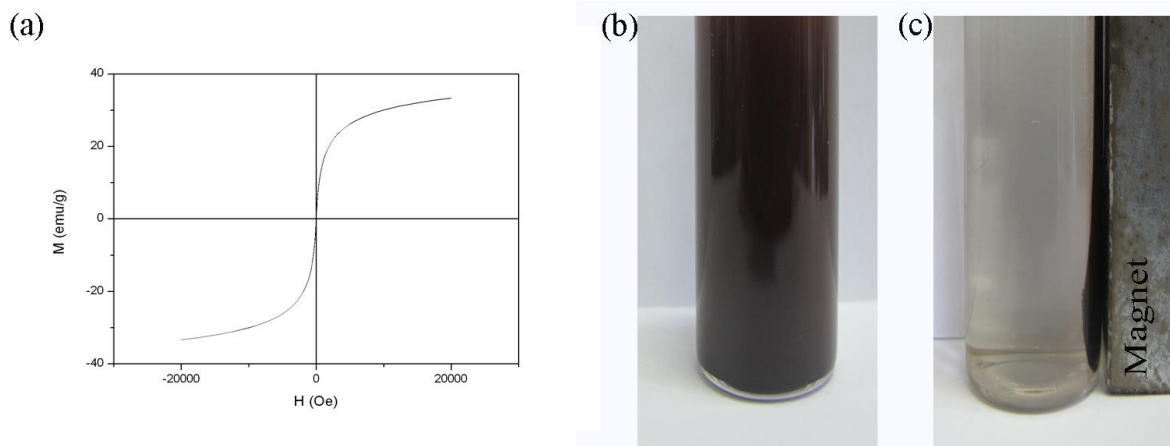


Fig. 4. (a) Magnetic hysteresis curves of MCCPs, and photographs of MCCPs suspended in water, (b) in the absence, and (c) in the presence of an externally placed magnet

Effect of pH

Solution pH is one of the dominant parameters affecting adsorption processes (Dogan *et al.* 2009). When the pH of the CR solution was reduced to below 4, its color changed from red to blue. Thus, the effect of the solution pH on CR adsorption capacity for a pH range of 5 to 10 was studied. As Fig. 5 shows, the effect of pH on CR adsorption was obvious in the initial stages of the adsorption process.

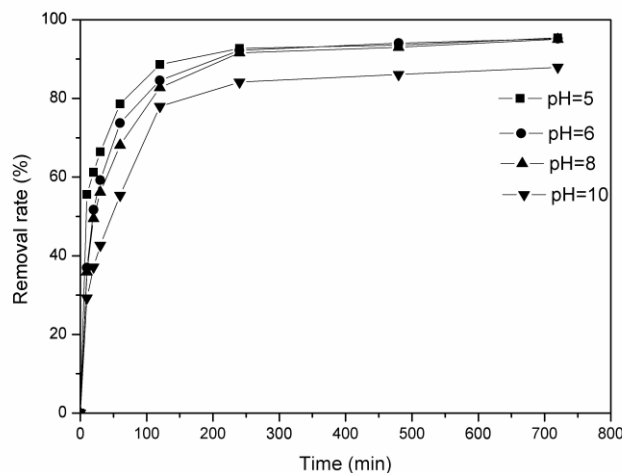


Fig. 5. Effect of initial solution pH for the adsorption of CR onto MCCPs (initial CR concentration: 50 mg L⁻¹, 50 mL, adsorbent dose: 30 mg, temperature: 30 °C)

The removal efficiency declined as the pH increased. When the adsorption reached equilibrium, the removal rate did not greatly differ between pH 5, pH 6, and pH 8, while the rate was lower for pH 10. During the initial stages of adsorption, a high concentration of hydrogen in the solution led to protonation of the amine groups in the chitosan chain, causing enhanced electrostatic interactions between the CR anions and chitosan (Kyzas and Lazaridis 2009). When the hydrogen atoms (H^+) were nearly consumed at equilibrium, the protonation of amine groups was not effective because of the low concentration of free H^+ in the solution. Nevertheless, for highly alkaline conditions, no free amino groups of chitosan could be protonated and the abundant OH^- competed with the dye anions (Chatterjee *et al.* 2005), resulting in decreased CR removal efficiency.

Effect of Initial CR Concentration

Figure 6 shows the adsorption capacities of CR onto MCCPs at various concentrations for different contact times. It is clear that the adsorption increased in the first 120 min, after which the adsorption slowed down, eventually approaching equilibrium at 480 min. The adsorption capacity increased as the initial dye concentration increased from 40 mg L⁻¹ to 70 mg L⁻¹. This behavior may be caused by the increase in the mass concentration gradient pressure as the initial concentration is increased. The initial dye concentration provides the necessary driving force to transfer the CR molecules from the bulk solution to the surface of the MCCPs (Senthil Kumar *et al.* 2010).

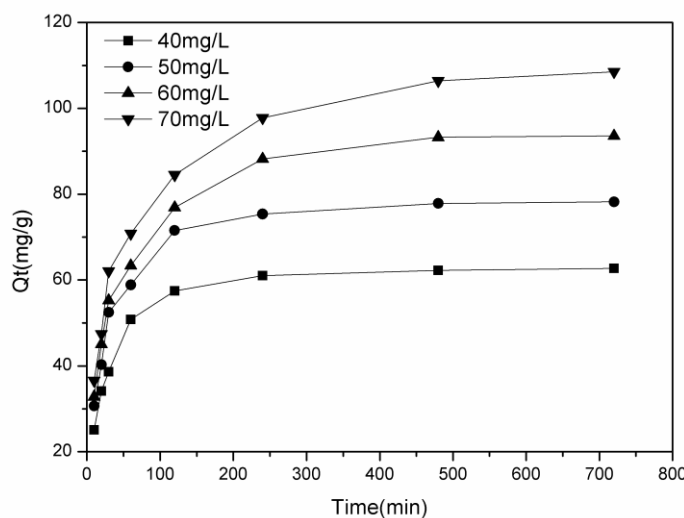


Fig. 6. Effect of initial dye concentration on the adsorption of CR onto MCCPs (adsorbent dose: 30 mg, temperature: 30 °C)

Adsorption Kinetics

The kinetic parameters of adsorption help predict the dominant adsorption mechanism and the adsorption rate of the adsorbate (Chen *et al.* 2009). Two simplified kinetic models, including Lagergren pseudo-first-order and pseudo-second-order equations, were used to fit the adsorption kinetic data.

The Lagergren pseudo-first-order model is given as (Ho and McKay 1998),

$$\ln(q_e - q_t) = \ln q_e - k_1 t \quad (2)$$

where q_e and q_t are the amounts of CR adsorbed (mg g^{-1}) at equilibrium and at time t (min), respectively, and k_1 is the Lagergren pseudo-first-order rate constant (min^{-1}) of adsorption. Values of k_1 can be calculated from plots of $\ln(q_e - q_t)$ versus t , as shown in Fig. 7(a).

The pseudo-second-order model is expressed as (Ho and McKay 1999),

$$\frac{t}{q_t} = \frac{1}{k_2 q_e^2} + \frac{t}{q_e} \quad (3)$$

where k_2 is the pseudo-second-order rate constant ($\text{g mg}^{-1} \text{ min}^{-1}$). Values of k_2 and q_e can be directly obtained from the intercept and slope of the plot of t/q_t versus t , as shown in Fig. 7(b).

The kinetic parameters of CR adsorption onto the MCCPs for different CR initial concentrations at 303 K are shown in Table 1.

Table 1. Kinetic Parameters for CR Adsorption onto MCCPs

| C_0 (mg L^{-1}) | $q_{e,\text{exp}}$ (mg g^{-1}) | Lagergren pseudo-first-order model | | | | pseudo-second-order model | | | |
|---------------------------------|--|---|------------------------|--|--------|---|------------------------|--|--------|
| | | $q_{1e,\text{cal}}$ (mg g^{-1}) | Change of q_e (%) | $k_1 \times 10^3$ (min^{-1}) | R^2 | $q_{2e,\text{cal}}$ (mg g^{-1}) | Change of q_e (%) | $k_2 \times 10^4$ ($\text{g mg}^{-1} \text{ min}^{-1}$) | R^2 |
| 40 | 62.71 | 26.38 | -57.93 | 9.20 | 0.9325 | 64.10 | 2.21 | 9.60 | 0.9999 |
| 50 | 78.20 | 36.84 | -52.89 | 10.00 | 0.9712 | 80.00 | 2.30 | 7.20 | 0.9999 |
| 60 | 93.57 | 61.11 | -34.69 | 10.90 | 0.9967 | 97.09 | 3.76 | 4.11 | 0.9997 |
| 70 | 108.54 | 65.48 | -39.67 | 7.30 | 0.9921 | 112.36 | 3.52 | 2.84 | 0.9991 |

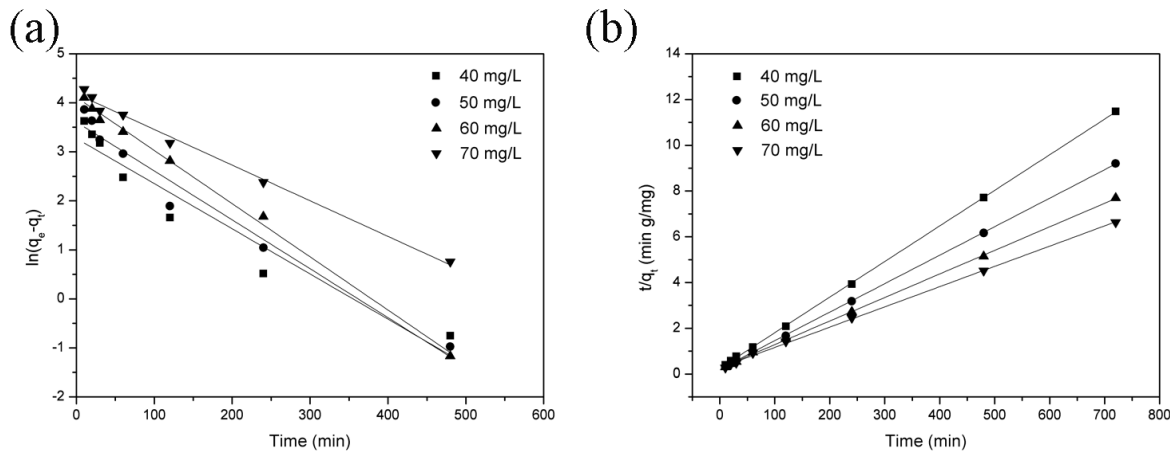


Fig. 7. Fitting curves of (a) pseudo-first-order model and (b) pseudo-second-order model for CR adsorption onto MCCPs at 303 K

The coefficients of determination (R^2) for the pseudo-second-order kinetic model were high (> 0.999), and the adsorption capacities calculated by the model ($q_{e,cal}$) were also close to those determined by experiments ($q_{e,exp}$). The pseudo-first-order model did not perform as well as the pseudo-second-order model, suggesting that the pseudo-second-order kinetic model was more valid for describing this adsorption process. Thus, chemical adsorption is the rate-limiting step of the adsorption mechanism (Fan *et al.* 2012a). Additionally, the values of the pseudo-second-order rate constants (k_2) increased as the initial CR concentration decreased, indicating that the adsorption reaction is more favorable for low initial CR concentrations.

Most adsorption processes have multiple steps, including surface diffusion and intraparticle diffusion (Zhu *et al.* 2011b). To determine whether intraparticle diffusion was the rate-determining step, the intraparticle mass transfer diffusion model was applied and expressed as (Wu *et al.* 2001),

$$q_t = k_{id} t^{1/2} + c \quad (4)$$

where c is the intercept (mg g^{-1}) and k_{id} is the intraparticle diffusion rate constant ($\text{mg g}^{-1} \text{min}^{-1/2}$), which can be evaluated from the slope of the linear plot of q_t versus $t^{1/2}$.

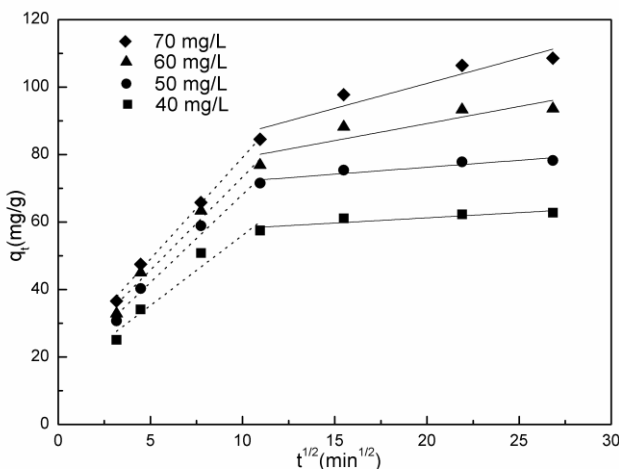


Fig. 8. Intraparticle diffusion plots for adsorption of CR onto MCCPs at 303 K

A plot of q_t versus $t^{1/2}$ is shown in Fig. 8. The adsorption process tended to have two phases: the initial curved portion and the second linear portion. The curved portion of the plot was attributed to surface adsorption and external diffusion, indicating a boundary-layer effect, whereas the linear portion was ascribed to intraparticle or pore diffusion (Zhu *et al.* 2011b). The linear portions of the curves at each concentration did not pass through the origin, suggesting that intraparticle diffusion was not the sole rate-limiting step (Bayramoglu *et al.* 2009). Additionally, the intercept value decreased with increasing initial CR concentration, indicating a decrease in the thickness of the boundary layer and its effect on adsorption.

Adsorption kinetics of CR onto MCCPs was better described by the pseudo-second-order model. The rate constants of the pseudo-second-order model were adopted

to calculate the activation energy of the adsorption process by the following Arrhenius equation (Konicki *et al.* 2013),

$$\ln k_2 = \ln A - \frac{E_a}{RT} \quad (5)$$

where k_2 ($\text{g mg}^{-1} \text{ min}^{-1}$) is the pseudo-second-order rate constant, A ($\text{g mg}^{-1} \text{ min}^{-1}$) is the Arrhenius factor, E_a (J mol^{-1}) is the Arrhenius activation energy, R ($8.314 \text{ J mol}^{-1} \text{ K}^{-1}$) is the gas constant, and T (K) is the absolute temperature. Plotting $\ln k_2$ as a function of $1/T$ (Fig. 9) yielded a straight line, from which E_a and A can be calculated using the slope and intercept, respectively. The magnitude of the activation energy gives an idea of the type of adsorption, which is primarily either physical or chemical. The physisorption process normally has a low activation energy (5 to 40 kJ mol^{-1}), while chemisorption has a higher activation energy (40 to 800 kJ mol^{-1}). The value of E_a for the adsorption CR onto MCCPs was 25.50 kJ mol^{-1} ($R^2 = 0.958$), indicating that the adsorption had a low potential barrier and corresponded to physisorption. Similar results have been observed for the adsorption of Acid Red 88 onto magnetic ZnFe_2O_4 spinel ferrite nanoparticles (37.5 kJ mol^{-1}) (Konicki *et al.* 2013).

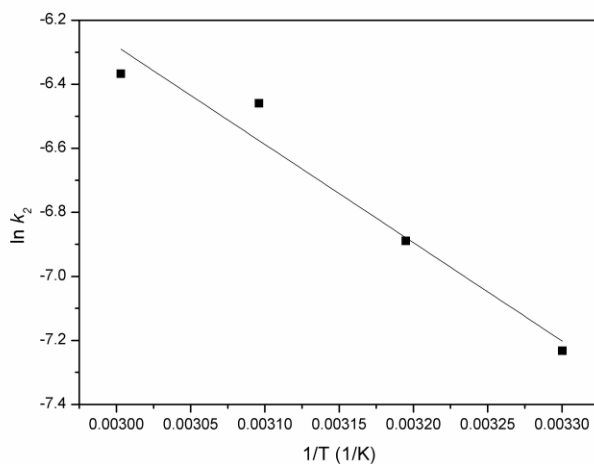


Fig. 9. Arrhenius plot for the adsorption of CR onto MCCPs

Adsorption Isotherms

Adsorption isotherm models are widely used to describe the interactions between adsorbates and adsorbents. Two well-known adsorption isotherms models, the Langmuir and Freundlich isotherms, have been used to study adsorption. The Langmuir and Freundlich isotherms can be respectively expressed as follows (Zhu *et al.* 2010),

$$\frac{C_e}{q_e} = \frac{1}{K_L q_m} + \frac{C_e}{q_m} \quad (6)$$

$$\ln q_e = \ln K_F + \frac{1}{n} \ln C_e \quad (7)$$

where C_e is the equilibrium concentration of CR in solution (mg L^{-1}); q_e is the adsorbed value of CR at equilibrium concentration (mg g^{-1}); q_m is the maximum adsorption capacity; K_L is the Langmuir adsorption constant, which is related to the energy of adsorption (L mg^{-1}); and K_F and n are the Freundlich constants related to the adsorption capacity and the surface heterogeneity, respectively.

Plotting C_e/q_e against C_e gave a straight line with a slope and intercept equal to $1/q_m$ and $1/(K_L q_m)$, respectively. The slope and intercept of the linear plots of $\ln q_e$ against $\ln C_e$ were $1/n$ and $\ln K_F$, respectively. The calculated Langmuir and Freundlich isotherm constants for CR adsorption at 303 K, 313 K, and 323 K are summarized in Table 2. As the R^2 values indicate, the Langmuir isotherm better described the adsorption of CR onto the MCCPs *versus* the Freundlich isotherm. This result shows that CR was adsorbed on the MCCPs by a monolayer adsorption process (Fan *et al.* 2012a). Notably, the adsorption capacity increased with temperature, showing that the adsorption process was endothermic.

The essential feature of the Langmuir isotherm can be described by a separation factor (R_L) using the following equation (Qi and Xu 2004),

$$R_L = \frac{1}{1 + K_L C_0} \quad (8)$$

where K_L is the Langmuir constant (L mg^{-1}) and C_0 is the initial concentration (mg L^{-1}). The range $0 < R_L < 1$ indicates that adsorption is favored. The values of R_L for the MCCPs toward the adsorption of CR at 303 K, 313 K, and 323 K are 0.114, 0.085, and 0.127, respectively; these values indicate that the adsorption of CR onto MCCPs is favorable.

Table 2. Langmuir and Freundlich Isotherm Constants at Different Temperatures

| T (K) | Langmuir isotherm constants | | | | Freundlich isotherm constants | | |
|---------|------------------------------|-------|-------|--------|--|------|--------|
| | q_m (mg g^{-1}) | K_L | R_L | R^2 | K_F ($\text{mg}^{1-(1/n)} \text{L}^{1/n} \text{g}^{-1}$) | n | R^2 |
| 303 | 181.82 | 0.155 | 0.114 | 0.9852 | 48.97 | 2.99 | 0.9335 |
| 313 | 208.33 | 0.214 | 0.085 | 0.9937 | 57.63 | 2.78 | 0.8685 |
| 323 | 263.16 | 0.137 | 0.127 | 0.9895 | 50.84 | 2.26 | 0.9041 |

Adsorption Thermodynamics

Thermodynamic parameters such as enthalpy change (ΔH°), entropy change (ΔS°), and Gibbs free energy change (ΔG°) were studied to determine the adsorption spontaneity and understand the effect of temperature on the adsorption. Thermodynamic experiments were conducted at 303, 313, 323, and 333 K, with a 50-mg L^{-1} initial CR concentration and a 30-mg adsorbent dosage. These thermodynamic parameters can be calculated using the following equations (Smith and Van Ness 1987),

$$\Delta G^\circ = -RT\ln K_c \quad (9)$$

$$\ln K_c = \frac{-\Delta H^\circ}{RT} + \frac{\Delta S^\circ}{R} \quad (10)$$

$$K_c = \frac{c_s}{c_e} \quad (11)$$

where K_c , the equilibrium constant, is the ratio of the concentration of CR on the adsorbent at equilibrium (c_s) to the remaining concentration of the dye in solution at equilibrium (c_e); ΔG^θ (kJ mol⁻¹), ΔH^θ (kJ mol⁻¹), and ΔS^θ (J mol⁻¹K⁻¹) are the changes in Gibbs free energy, enthalpy, and entropy, respectively; R is the ideal gas constant (8.314 J mol⁻¹K⁻¹); and T is the absolute temperature (K).

Plotting $\ln K_c$ against $1/T$ gave a straight line with a slope and intercept equal to $\Delta H^\theta/R$ and $\Delta S^\theta/R$, respectively. The values of ΔG^θ , ΔH^θ , and ΔS^θ are listed in Table 3. The negative ΔG^θ values imply spontaneous adsorption. The positive value of ΔS^θ suggests increased randomness during the adsorption of CR. The positive value of ΔH^θ shows that the adsorption process was endothermic; therefore, higher temperatures will facilitate the adsorption of CR onto the MCCPs, which is consistent with the results of the adsorption isotherms.

Table 3. Thermodynamic Parameters for the Adsorption of CR onto MCCPs

| T (K) | ΔG^θ (kJ mol ⁻¹) | $T\Delta S^\theta$ (kJ mol ⁻¹) | ΔH^θ (kJ mol ⁻¹) | ΔS^θ (J mol ⁻¹ K ⁻¹) |
|-------|---|--|---|--|
| 303 | -6.863 | 20.603 | | |
| 313 | -7.932 | 21.283 | 13.598 | 67.998 |
| 323 | -8.320 | 21.963 | | |
| 333 | -8.982 | 22.643 | | |

Comparison with Other Adsorbents

The maximum adsorption capacity (q_{max}) of CR onto the MCCPs from the Langmuir isotherm was calculated. This was then compared with those of other biosorbents reported by other researchers; these data are listed in Table 4. The table shows that the q_{max} value of the MCCPs was generally higher than those of other chitosan-based adsorbents (Chatterjee *et al.* 2007; Wang and Wang 2007b; Chatterjee *et al.* 2009), and cellulose-based adsorbents (Annadurai *et al.* 2002; Panda *et al.* 2009; Zhu *et al.* 2011a), except for the chitosan/organo-montomorillonite adsorbent (Wang and Wang 2007a). However, the simplicity of the MCCP preparation process and their magnetic properties make them more suitable for CR adsorption.

Table 4. q_{max} Values for the Adsorption of CR on Different Adsorbents

| Adsorbent | q_{max} (mg/g) | Reference |
|---|------------------|-------------------------------|
| Chitosan beads | 93.71 | Chatterjee <i>et al.</i> 2007 |
| Chitosan powder | 74.73 | Wang and Wang 2007 |
| Chitosan/montmorillonite nanocomposite | 54.52 | Wang and Wang 2007 |
| Chitosan/SDS beads | 223.25 | Chatterjee <i>et al.</i> 2009 |
| Chitosan/organo-montomorillonite | 290.80 | Wang and Wang, 2007 |
| Magnetic cellulose/Fe ₃ O ₄ /activated carbon composite | 66.09 | Zhu <i>et al.</i> 2011a |
| Jute stick power | 35.70 | Panda <i>et al.</i> 2009 |
| Banana peel | 18.20 | Annadurai <i>et al.</i> 2002 |
| Orange peel | 14.00 | Annadurai <i>et al.</i> 2002 |
| MCCPs | 263.16 | This work |

Regeneration of MCCPs

The regeneration of spent adsorbent is considered an important economical aspect to minimize the cost of the adsorption process. In this study, 0.5 M NaOH was selected as the eluent for desorption; after desorption, the MCCPs were washed with deionized water and 0.5 M HCl until the residual solution became colorless. Then, the recovered adsorbents were used for the next loading cycle. The regeneration studies were repeated seven times, and the results are shown in Fig. 10. It can be seen that the adsorption capacity decreased slightly with increasing cycles. In the first three cycles, the adsorption efficiency of the MCCPs remained almost constant: after being regenerated five times, the removal rate of CR was still more than 80%. This fact indicates that the MCCPs can be used as a reusable adsorbent for CR adsorption from aqueous solution.

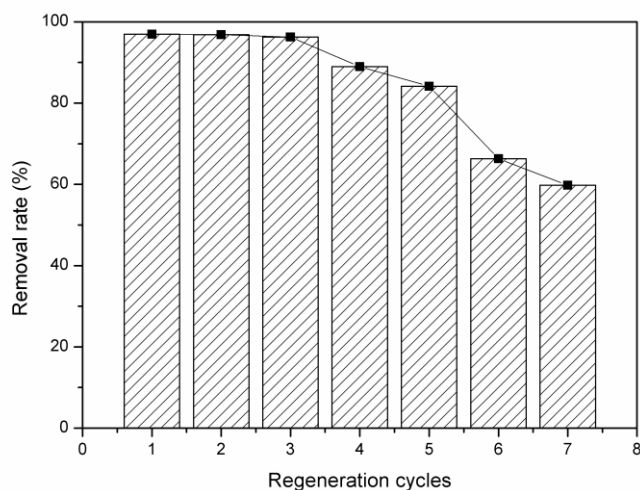


Fig. 10. Effect of regeneration cycles on CR adsorption (initial CR concentration: 50 mg L⁻¹, 50 mL, adsorbent dose: 30 mg, temperature: 30 °C)

CONCLUSIONS

1. Magnetic chitosan composite microparticles were prepared with a simple one-step co-precipitation method; they had a honeycomb-like porous structure and were superparamagnetic.
2. The FT-IR spectra revealed that the chitosan was bound to the magnetic Fe₃O₄ microparticles successfully without damaging the crystal structure of Fe₃O₄.
3. The removal efficiency increased as the initial concentration increased and as the pH declined in the range from 10 to 5.
4. The adsorption process was best described by a pseudo-second-order equation, and equilibrium experiments agreed well with the Langmuir isotherm model.
5. Thermodynamic calculations indicated that the adsorption process was spontaneous and endothermic.
6. The MCCPs have a great potential to be used as an environmentally friendly and economical adsorbent for removal of CR from aqueous solution.

ACKNOWLEDGMENTS

The authors gratefully acknowledge the Fundamental Research Funds for the Central Universities (DL12DB04).

REFERENCES CITED

- Abou El-Reash, Y. G., Otto, M., Kenawy, I. M., and Ouf, A. M. (2011). "Adsorption of Cr(VI) and As(V) ions by modified magnetic chitosan chelating resin," *Int. J. Bio. Macromol.* 49(4), 513-522.
- Annadurai, G., Juang, R., and Lee, D. (2002). "Use of cellulose-based wastes for adsorption of dyes from aqueous solutions," *J. Hazard. Mater.* 92(3), 263-274.
- Barragán, B. E., Costa, C., and Carmen Márquez, M. (2007). "Biodegradation of azo dyes by bacteria inoculated on solid media," *Dyes Pigments* 75(1), 73-81.
- Bayramoglu, G., Altintas, B., and Arica, M. Y. (2009). "Adsorption kinetics and thermodynamic parameters of cationic dyes from aqueous solutions by using a new strong cation-exchange resin," *Chem. Eng. J.* 152(2-3), 339-346.
- Bromley-Challenor, K. (2000). "Decolorization of an azo dye by unacclimated activated sludge under anaerobic conditions," *Water Res.* 34(18), 4410-4418.
- Chatterjee, S., Chatterjee, S., Chatterjee, B. P., Das, A. R., and Guha, A. K. (2005). "Adsorption of a model anionic dye, eosin Y, from aqueous solution by chitosan hydrobeads," *J. Colloid Interface Sci.* 288(1), 30-35.
- Chatterjee, S., Chatterjee, S., Chatterjee, B. P., and Guha, A. K. (2007). "Adsorptive removal of Congo red, a carcinogenic textile dye by chitosan hydrobeads: Binding mechanism, equilibrium and kinetics," *Colloids Surf. A: Physicochem. Eng. Aspects* 299(1-3), 146-152.
- Chatterjee, S., Lee, D. S., Lee, M. W., and Woo, S. H. (2009). "Congo red adsorption from aqueous solutions by using chitosan hydrogel beads impregnated with nonionic or anionic surfactant," *Bioresour. Technol.* 100(17), 3862-3868.
- Chen, G. C., Shan, X. Q., Zhou, Y. Q., Shen, X. E., Huang, H. L., and Khan, S. U. (2009). "Adsorption kinetics, isotherms and thermodynamics of atrazine on surface oxidized multiwalled carbon nanotubes," *J. Hazard. Mater.* 169(1-3), 912-918.
- Crini, G., and Badot, P. M. (2008). "Application of chitosan, a natural aminopolysaccharide, for dye removal from aqueous solutions by adsorption processes using batch studies: A review of recent literature," *Pro. Polym. Sci.* 33(4), 399-447.
- Dogan, D. A., and Türkdemir, H. (2005). "Electrochemical oxidation of textile dye indigo," *J. Chem. Technol. Biotechnol.* 80(8), 916-923.
- Dogan, M., Abak, H., and Alkan, M. (2009). "Adsorption of methylene blue onto hazelnut shell: Kinetics, mechanism and activation parameters," *J. Hazard. Mater.* 164(1), 172-181.
- Donia, A. M., Atia, A. A., and Elwakeel, K. Z. (2008). "Selective separation of mercury(II) using magnetic chitosan resin modified with Schiff's base derived from thiourea and glutaraldehyde," *J. Hazard. Mater.* 151(2-3), 372-379.
- Elwakeel, K. Z. (2010). "Removal of Cr(VI) from alkaline aqueous solutions using chemically modified magnetic chitosan resins," *Desalination* 250(1), 105-112.
- Ertugay, N., and Acar, F. N. (2013). "Removal of COD and color from direct blue 71 azo dye wastewater by Fenton's oxidation: Kinetic study," *Arab. J. Chem.* (in press) doi: <http://dx.doi.org/10.1016/j.arabjc.2013.02.009>.

- Fan, L., Luo, C., Sun, M., Qiu, H., and Li, X. (2013). "Synthesis of magnetic β -cyclodextrin–chitosan/graphene oxide as nanoadsorbent and its application in dye adsorption and removal," *Colloids Surf. B: Biointerfaces* 103(1), 601-607.
- Fan, L., Zhang, Y., Li, X., Luo, C., Lu, F., and Qiu, H. (2012a). "Removal of alizarin red from water environment using magnetic chitosan with alizarin red as imprinted molecules," *Colloids Surf. B: Biointerfaces* 91, 250-257.
- Fan, L., Zhang, Y., Luo, C., Lu, F., Qiu, H., and Sun, M. (2012b). "Synthesis and characterization of magnetic β -cyclodextrin-chitosan nanoparticles as nano-adsorbents for removal of methyl blue," *Int. J. Biol. Macromol.* 50(2), 444-450.
- Gupta, V. K., Carrott, P. J. M., Ribeiro Carrott, M. M. L., and Suhas. (2009). "Low-cost adsorbents: Growing approach to wastewater treatment - A review," *Crit. Rev. Env. Sci. Technol.* 39(10), 783-842.
- Gupta, V. K., Jain, R., and Varshney, S. (2007). "Electrochemical removal of the hazardous dye Reactofix Red 3 BFN from industrial effluents," *J. Colloid Interface Sci.* 312(2), 292-296.
- Hage, R., and Lienke, A. (2005). "Applications of transition-metal catalysts to textile and wood-pulp bleaching," *Angew. Chem. Int. Ed.* 45(2), 206-222.
- Ho, Y. S., and McKay, G. (1998). "A comparison of chemisorption kinetic models applied to pollutant removal on various sorbents," *Process Saf. Environ. Prot.* 76(4), 332-340.
- Ho, Y. S., and McKay, G. (1999). "Pseudo-second order model for sorption processes." *Process Biochem.* 34(5), 451-465.
- Jia, B., Zhou, J., and Zhang, L. (2011). "Electrospun nano-fiber mats containing cationic cellulose derivatives and poly (vinyl alcohol) with antibacterial activity," *Carbohydr. Res.* 346(11), 1337-41.
- Khatri, Z., Mayakrishnan, G., Hirata, Y., Wei, K., and Kim, I. S. (2013). "Cationic-cellulose nanofibers: Preparation and dyeability with anionic reactive dyes for apparel application," *Carbohydr. Polym.* 91(1), 434-43.
- Konicki, W., Siber, D., Mijowska, E., Lendzion-Bielun, Z., and Narkiewicz, U. (2013). "Equilibrium and kinetic studies on acid dye acid red 88 adsorption by magnetic $ZnFe_2O_4$ spinel ferrite nanoparticles," *J. Colloid Interface Sci.* 398, 152-160.
- Kyzas, G. Z., and Deliyanni, E. A. (2013). "Mercury(II) removal with modified magnetic chitosan adsorbents," *Molecules* 18(6), 6193-214
- Kyzas, G. Z., and Lazaridis, N. K. (2009). "Reactive and basic dyes removal by sorption onto chitosan derivatives," *J. Colloid Interface Sci.* 331(1), 32-39
- Lee, H. C., Jeong, Y. G., Min, B. G., Lyoo, W. S., and Lee, S. C. (2009). "Preparation and acid dye adsorption behavior of polyurethane/chitosan composite foams," *Fiber. Polym.* 10(5), 636-642.
- Lee, H. S., Kim, E. H., Shao, H. P., and Kwak, B. K. (2005). "Synthesis of SPIO-chitosan microspheres for MRI-detectable embolotherapy," *J. Magn. Magn. Mater.* 293(1), 102-105.
- Li, G. Y., Jiang, Y. R., Huang, K. L., Ding, P., and Chen, J. (2008). "Preparation and properties of magnetic Fe_3O_4 -chitosan nanoparticles," *J. Alloys Compd.* 466(1-2), 451-456.
- Li, H., Bi, S., Liu, L., Dong, W., and Wang, X. (2011). "Separation and accumulation of Cu(II), Zn(II) and Cr(VI) from aqueous solution by magnetic chitosan modified with diethylenetriamine," *Desalination* 278(1-3), 397-404.

- Lin, H., Lu, Q., Ge, S., Cai, Q., and Grimes, C.A. (2010). "Detection of pathogen *Escherichia coli* O157:H7 with a wireless magnetoelastic-sensing device amplified by using chitosan-modified magnetic Fe_3O_4 nanoparticles," *Sens. Actuators, B* 147(1), 343-349.
- Lin, S. H., Juang, R. S., and Wang, Y. H. (2004). "Adsorption of acid dye from water onto pristine and acid-activated clays in fixed beds," *J. Hazard. Mater.* 113(1-3), 195-200.
- Liu, C. H., Wu, J. S., Chiu, H. C., Suen, S. Y., and Chu, K. H. (2007). "Removal of anionic reactive dyes from water using anion exchange membranes as adsorbers," *Water Res.* 41(7), 1491-1500.
- Liu, Y., Jia, S., Wu, Q., Ran, J., Zhang, W., and Wu, S. (2011). "Studies of Fe_3O_4 -chitosan nanoparticles prepared by co-precipitation under the magnetic field for lipase immobilization," *Catal. Commun.* 12(8), 717-720.
- Ma, W., Ya, F. Q., Han, M., and Wang, R. (2007). "Characteristics of equilibrium, kinetics studies for adsorption of fluoride on magnetic-chitosan particle," *J. Hazard. Mater.* 143(1-2), 296-302.
- Mishra, A., and Bajpai, M. (2006). "The flocculation performance of Tamarindus mucilage in relation to removal of vat and direct dyes," *Bioresour. Technol.* 97(8), 1055-1059.
- Mohan, S. V., Rao, N. C., and Karthikeyan, J. (2002). "Adsorptive removal of direct azo dye from aqueous phase onto coal based sorbents: A kinetic and mechanistic study," *J. Hazard. Mater.* 90(2), 189-204.
- Morais, L. C., Freitas, O. M., Gonçalves, E. P., Vasconcelos, L. T., and González Beça, C. G. (1999). "Reactive dyes removal from wastewaters by adsorption on eucalyptus bark: Variables that define the process," *Water Res.* 33(4), 979-988.
- Nandi, B. K., Goswami, A., and Purkait, M. K. (2009). "Adsorption characteristics of brilliant green dye on kaolin," *J. Hazard. Mater.* 161(1), 387-395.
- Ngah, W. S. W., and Isa, I. M. (1998). "Comparison study of copper ion adsorption on chitosan, Dowex A-1, and Zerolit 225," *J. Appl. Polym. Sci.* 67(6), 1067-1070.
- Ngah, W. S. W., Teong, L. C., and Hanafiah, M. A. K. M. (2011). "Adsorption of dyes and heavy metal ions by chitosan composites: A review," *Carbohydr. Polym.* 83(4), 1446-1456.
- Panda, G. C., Das, S. K., and Guha, A. K. (2009). "Jute stick powder as a potential biomass for the removal of congo red and rhodamine B from their aqueous solution," *J. Hazard. Mater.* 164(1), 374-379.
- Qi, L., and Xu, Z. (2004). "Lead sorption from aqueous solutions on chitosan nanoparticles," *Colloids Surf. A: Physicochem. Eng. Aspects* 251(1-3), 183-190.
- Qu, J., Liu, G., Wang, Y., and Hong, R. (2010). "Preparation of Fe_3O_4 -chitosan nanoparticles used for hyperthermia," *Adv. Powder Technol.* 21(4), 461-467.
- Raghu, S., and Ahmed Basha, C. (2007). "Chemical or electrochemical techniques, followed by ion exchange, for recycle of textile dye wastewater," *J. Hazard. Mater.* 149(2), 324-330.
- Rodríguez, R. A., Alvarez-Lorenzo, C., and Concheiro, A. (2003). "Cationic cellulose hydrogels: Kinetics of the cross-linking process and characterization as pH-/ion-sensitive drug delivery systems," *J. Controlled Release* 86(2-3), 253-265.
- Sani, R. K., and Banerjee, U. C. (1999). "Decolorization of triphenylmethane dyes and textile and dye-stuff effluent by *Kurthia* sp," *Enzyme Microb. Technol.* 24(7), 433-437.

- Senthil Kumar, P., Ramalingam, S., Senthamarai, C., Niranjanaa, M., Vijayalakshmi, P., and Sivanesan, S. (2010). "Adsorption of dye from aqueous solution by cashew nut shell: Studies on equilibrium isotherm, kinetics and thermodynamics of interactions," *Desalination* 261(1-2), 52-60.
- Shi, B., Li, G., Wang, D., Feng, C., and Tang, H. (2007). "Removal of direct dyes by coagulation: The performance of preformed polymeric aluminum species," *J. Hazard. Mater.* 143(1-2), 567-574.
- Sirviö, J., Honka, A., Liimatainen, H., Niinimäki, J., and Hormi, O. (2011). "Synthesis of highly cationic water-soluble cellulose derivative and its potential as novel biopolymeric flocculation agent," *Carbohydr. Polym.* 86(1), 266-270.
- Smith, J. M., and Van Ness, H. C. (1987). *Introduction to Chemical Engineering Thermodynamics*, 4th Ed., McGraw-Hill Book Company, New York.
- Srinivasan, A., and Viraraghavan, T. (2010). "Decolorization of dye wastewaters by biosorbents: A review," *J. Environ. Manage.* 91(10), 1915-1929.
- Sun, Q., and Yang, L. (2003). "The adsorption of basic dyes from aqueous solution on modified peat-resin particle," *Water Res.* 37(7), 1535-1544.
- Tan, I. A. W., Hameed, B. H., and Ahmad, A. L. (2007). "Equilibrium and kinetic studies on basic dye adsorption by oil palm fibre activated carbon," *Chem. Eng. J.* 127(1-3), 111-119.
- Tran, H. V., Tran, L. D., and Nguyen, T. N. (2010). "Preparation of chitosan/magnetite composite beads and their application for removal of Pb(II) and Ni(II) from aqueous solution," *Mater. Sci. Eng., C* 30(2), 304-310.
- Travlou, N.A., Kyzas, G.Z., Lazaridis, N.K., and Deliyanni, E.A. (2013). "Functionalization of graphite oxide with magnetic chitosan for the preparation of a nanocomposite dye adsorbent," *Langmuir* 29(5), 1657-1668.
- Wang, J. P., Chen, Y. Z., Ge, X. W., and Yu, H. Q. (2007a). "Optimization of coagulation-flocculation process for a paper-recycling wastewater treatment using response surface methodology," *Colloids Surf. A: Physicochem. Eng. Aspects* 302(1-3), 204-210.
- Wang, L., and Wang, A. Q. (2007b). "Removal of Congo red from aqueous solution using a chitosan/organo-montmorillonite nanocomposite," *J. Chem. Technol. Biotechnol.* 82(8), 711-720.
- Wang, L., and Wang, A. (2007c). "Adsorption characteristics of Congo red onto the chitosan/montmorillonite nanocomposite," *J. Hazard. Mater.* 147(3), 979-985.
- Wu, F. C., Tseng, R. L., and Juang, R. S. (2001). "Kinetic modeling of liquid-phase adsorption of reactive dyes and metal ions on chitosan," *Water Res.* 35(3), 613-618.
- Yan, H., Li, H., Yang, H., Li, A., and Cheng, R. (2013). "Removal of various cationic dyes from aqueous solutions using a kind of fully biodegradable magnetic composite microsphere," *Chem. Eng. J.* 223, 402-411.
- Yan, H., Yang, L., Yang, Z., Yang, H., Li, A., and Cheng, R. (2012). "Preparation of chitosan/poly(acrylic acid) magnetic composite microspheres and applications in the removal of copper(II) ions from aqueous solutions," *J. Hazard. Mater.* 229-230, 371-380.
- Yang, H., Li, Y., Ho, S. S., Tian, X., Xia, Y., Shen, Y., Zhao, M., and Pan, G. (2013). "Preparation and characterization of EDTAD-modified magnetic-Fe₃O₄ chitosan composite: Application of comparative adsorption of dye wastewater with magnetic chitosan," *Water Sci. Technol.* 68(1), 209-216.

- Yu, Z., Zhang, X., and Huang, Y. (2013). "Magnetic chitosan–iron(III) hydrogel as a fast and reusable adsorbent for chromium(VI) Removal," *Ind. Eng. Chem. Res.* 52(34), 11956-11966.
- Zhang, L. Y., Zhu, X. J., Sun, H. W., Chi, G. R., Xu, J. X., and Sun, Y. L. (2010). "Control synthesis of magnetic Fe_3O_4 –chitosan nanoparticles under UV irradiation in aqueous system," *Curr. Appl. Phys.* 10(3), 828-833.
- Zhu, H. Y., Fu, Y. Q., Jiang, R., Jiang, J. H., Xiao, L., Zeng, G. M., Zhao, S. L., and Wang, Y. (2011a). "Adsorption removal of congo red onto magnetic cellulose/ Fe_3O_4 /activated carbon composite: Equilibrium, kinetic and thermodynamic studies," *Chem. Eng. J.* 173(2), 494-502.
- Zhu, H. Y., Fu, Y. Q., Jiang, R., Yao, J., Xiao, L., and Zeng, G. M. (2012). "Novel magnetic chitosan/poly(vinyl alcohol) hydrogel beads: Preparation, characterization and application for adsorption of dye from aqueous solution," *Bioresour. Technol.* 105, 24-30.
- Zhu, H. Y., Jiang, R., Fu, Y. Q., Jiang, J. H., Xiao, L., and Zeng, G. M. (2011). "Preparation, characterization and dye adsorption properties of $\gamma\text{-Fe}_2\text{O}_3/\text{SiO}_2$ /chitosan composite," *Appl. Surf. Sci.* 258(4), 1337-1344.
- Zhu, H. Y., Jiang, R., Xiao, L., and Zeng, G. M. (2010). "Preparation, characterization, adsorption kinetics and thermodynamics of novel magnetic chitosan enwrapping nanosized $\gamma\text{-Fe}_2\text{O}_3$ and multi-walled carbon nanotubes with enhanced adsorption properties for methyl orange," *Bioresour. Technol.* 101(14), 5063-5069.

Article submitted: August 27, 2013; Peer review completed: September 28, 2013;
Revised version received and accepted: September 30, 2013; Published: October 3, 2013.